Early View publication on onlinelibrary.wiley.com
(issue and page numbers not yet assigned;
citable using Digital Object Identifier – **DOI**)

Phys. Status Solidi C, 1–5 (2010) / **DOI** 10.1002/pssc.201000110

physica status solidi c
www.pss-c.com
current topics in solid state physics

Influence of PECVD SiO_x and SiN_x:H films on optical and passivation properties of antireflective porous silicon coatings for silicon solar cells

L. Remache[*,1], A. Mahdjoub[2], E. Fourmond[1], J. Dupuis[1], and M. Lemiti[1]

[1] Institut des Nanotechnologies de Lyon INL, CNRS-UMR 5270, Université de Lyon, INSA-Lyon, Villeurbanne 69621, France
[2] Laboratoire LMSSEF, Université d'Oum El Bouaghi, BP 358, Algérie

Received 18 April 2010, revised 21 September 2010, accepted 21 September 2010
Published online 1 December 2010

Keywords porous silicon, silicon dioxide, silicon nitride, antireflection coating, passivation, photocurrent

* Corresponding author: e-mail rlouardi@yahoo.fr, Phone: +00213 472 43 60 79, Fax: +00213 472 43 60 79

The meso-porous silicon layer (PS) is a promising material to reduce the surface reflectance of solar cells. PS layers were grown on the front surface n^+ emitter of n^+-p mono-crystalline Si junction. Single layers PS antireflection coating (ARC) achieved around 8% of effective reflectivity in the wavelength range between 400 to 1100 nm. To improve the stability and the passivation properties, and to reduce the reflectivity of PS ARC, the design of PECVD silicon oxide (SiO_x) and silicon nitride (SiN_x:H) layers were investigated. Optimised SiO_x and SiN_x layer deposited on PS decreased the effective reflectivity respectively to ~3.8% and ~7% between 400 and 1000 nm. Open circuit voltage (V_{oc}) measurements were carried out on all the samples by suns-Voc method and showed an improvement of 20% of the surface passivation quality brought by the nitride layer after rapid thermal anneal (RTA). Using the experimental reflectivity results and taking into account the surface passivation quality of the samples, numerical simulations predict an enhancement of the photogenerated current exceeding 49% for the PS/SiO_x stacks.

1 Introduction Porous Silicon (PS) is a nanostructured material that has interesting applications in optoelectronics and photovoltaics [1-5]. Particulary it can be applied on silicon solar cells as an antireflection coating, due to low average reflectance values.
Conventionally, the PS layer has been formed by electrochemical etching and chemical etching [6]. The chemical method though being well adapted to mass production, present a major drawback. Menna et al [7] showed that within a given set of conditions, the simultaneous control of the PS parameters (thichness and porosity) is difficult to achieve. The electrochemical etching is advantageous for forming the PS layer under controlled conditions by adjusting the current density, which is a key formation parameter determining the PS porosity.
Recently, it has been shown that porous silicon antireflection coating (ARC) prepared by electrochemical etching on a laboratory solar cell could replace the texturization (random pyramids on mono-crystalline silicon or isotropic etching on micro-crystalline silicon). Indeed PS possesses some advantages: (i) better uniformity [4] (ii) create simultaneously a selective emitter and an antireflection coating [6-10] (iii) enlarge the spectral sensitivity region of the solar cell [6] and (iv) a better control of the parameters (porosity and thickness) leading to an optimum ARC [7].
However, the surface recombination velocity strongly increases when using PS layers, due to the roughness of the surface [11-13]. The optical properties of PS layers may also degrade in time when no further treatment is used, such as rapid thermal oxidation (RTO), nitridation, anodic oxidation, thermal carbonization [14-16]. These treatments may be efficient in terms of surface passivation, but exhibit many drawbacks: severe conditions of elaboration leading to the degradation of the porous silicon layer properties,

since these treatments generally imply a high temperature step [6]. In this context silicon nitride SiN_x:H and silicon oxide SiO_x films deposited by plasma enhanced CVD (PECVD) on porous silicon surface are of interest: (i) high chemical stability [16-18], (ii) good surface passivation before and after annealing [19,20], (iii) refractive indexes suitable for low reflectance antireflection coating (iv) and deposition by a low thermal process (PECVD) on PS, without deteriorating the optical and structural properties of the underlying PS [17,21].

This work aims to study the impact of the SiN_x and the SiO_x layers on the surface passivation of the PS layers. The technical method used for the front contact metallization on the PS layer was not optimised, and led to the degradation of the electrical quality of the metal contact. We have thus preferred to characterise the influence of the dielectric layers on the surface PS by using an indirect method: the measurement of the implied open circuit voltage V_{oc}. This was measured by the Sinton Suns-V_{oc} method [22], and gives information on the surface passivation quality.

2 Experimental The experiments were carried out on CZ (100) p-type silicon substrates, with a bulk resistivity of 1-10 Ωcm. The emitter was created by diffusion at 850 °C for 20 min, in an open quartz tube using liquid $POCl_3$ as the doping source. This results in a sheet resistance of 45 Ω/□. The junction depth in both cases was around 0.3 µm. After diffusion the parasitic junction and the phosphorus silicate glass were removed in dilute HF. In order to allow homogeneous electrochemical porosification of the silicon surface, an aluminum layer was evaporated under vacuum on the back side of the sample and was subsequently annealed in air at 750 °C to establish an ohmic contact. This Al back contact was connected to a constant current source. PS was grown on the front polished side by using a solution of HF (48%) and C_2H_5OH (3:1 or 4:1 in volume) in a Teflon electrochemical anodization cell. A platinum wire was used as a cathode at a distance of 2 cm from the Si wafer surface, which acted as the anode. In order to grow PS layers with different thicknesses, a set of experiments was performed by using a constant current density of 20 mA/cm^2 during different anodization time: 3.5 to 12 s. SiO_x and/or SiN_x films were then deposited in a vertical semi-industrial low Frequency PECVD reactor (LF – PECVD) at 440 kHz from SEMCO Engineering (described in [23]), using pure silane (SiH_4) and nitrous oxide (N_2O) or silane and ammonia (SiH_4, NH_3) as precursors gases. The deposition was made on the PS surface freshly prepared, at 370 °C with a power density of 0.26 W/cm^2, a pressure of 1500 mTorr, and a N_2O/SiH_4 gas flow ratio equal to 25 for SiO_x, and NH_3/SiH_4 gas flow ratio equal to 5 for SiN_x:H.

In order to optimize the ARC parameters (optical indexes and thicknesses), simulations based on the stratified medium theory and the Bruggeman effective medium approximation (EMA) [24], are carried out in the wavelength range between 350 and 1100 nm. The PC1D software was used to estimate the expected values of the photocurrent of the solar cells [25]. The PS thickness and porosity, the oxide and nitride thicknesses were measured by a Jobin Yvon Uvisel Ellipsometer using the Bruggemann effective medium approximation model (EMA) in the range of 1.5 to 5 eV. The total reflectance was measured within the 400–1100 nm wavelength range with an integrating sphere. The effective reflectance (R_{eff}) is calculated by integrating the reflectivity values balanced by the Sun global irradiance (AM1.5g spectrum). The front side metallization of the solar cells was made by evaporation of Ti/Pd/Ag contacts followed by a sintering step in air at 450 °C. The photovoltaic pseudo-parameters (open circuit voltage V_{oc} and pseudo Fill-Factor FF) were measured using a Sinton Suns-Voc Stage model WCT-120.

3 Results and discussion

3.1 Optical results

3.1.1 A porous silicon layer Three essential parameters are used to optimize the antireflection properties of porous silicon: the HF concentration in the ethanol, the current density and the anodization time. In our case two solutions are used: HF (48%): C_2H_5OH = 3:1 or 4:1 in volume. To obtain the adequate refractive index for the PS, the current density is fixed at 5mA/cm^2 or 20mA/cm^2, and the thickness of the layer is controlled by the anodization duration. Figure 1 shows the variation of thicknesses according to the anodization time. We notice that the thicknesses are very sensitive to the variations of the anodization time using 20mA/cm^2 as the current density. The average growth kinetics is around 14nm/s. However the thickness varies slightly versus the anodization time when the current density is fixed at 5mA/cm^2. Our calculations showed that the optimum thickness of the antireflection coating (ARC PS) is 80 nm, which corresponds to 6s (J = 20 mA/cm^2) of anodization time.

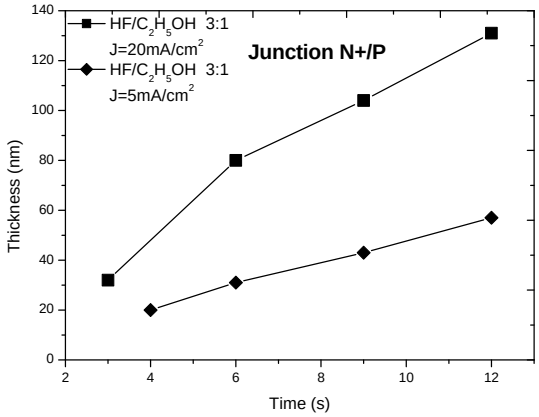

Figure 1 Thickness E vs time t of PS growth at a constant current density of 5 mAcm^{-2} and 20 mAcm^{-2} on n^+ diffused side of (100) Si wafer.

The reflectivity curves of the PS grown on the diffused emitter with a current density of 20mA/cm^2 and in electrolyte concentrations HF/C_2H_5OH of 3:1 and 4:1 are represented in Fig. 2. The best reflectance is obtained with the second solution, and presents an effective reflectivity of 8 % (between 400 and 1000 nm) with a minimum (R ~ 0)

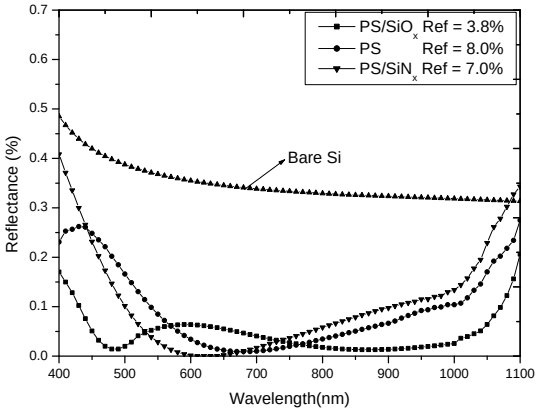

Figure 3 Reflectance spectra of PS/SiO_x , PS/SiN_x films on n+/p junction compared to as-grown PS.

at the wavelength of 650 nm. This solution allows to obtain the expected value of porosity which leads exactly to the adequate refractive index, leading to the optimization of ARC PS layer. The effective reflectivity compared to that of the standard ARC nitride (R=NH_3/SiH_4=5) is improved by 1 % absolute.

3.1.2 B PS/SiN_x and PS/SiO_x structures In order to improve the reflectivity of a single ARC PS, a double PS layer can be grown on the top of the silicon n^+/p junction. However this kind of coating can lead to a degradation of the n^+ emitter by reducing its thickness, and do not insure a good surface passivation. The deposition of a silicon nitride (SiN_x:H) and a silicon oxide (SiO_x) layers over to the PS layer may be an alternative solution. The silicon oxides and the silicon nitrides deposited in our reactor LF-PECVD present a large range of refractive indexes (respectively between n=1.47-2 and n=1.84-3 at λ=633 nm), and present also a very weak absorption in the range 300-1100 nm. These layers can thus be used on the top of the PS layer, to realize refractive index adaptation for reflection minimisation. Using the simulation methods based on the stratified medium theory and the Bruggeman effective medium approximation (EMA) [24], we have optimized thicknesses for both SiN_x and SiO_x layers (45 nm and 105 nm respectively). Experimental reflectivity results obtained after deposition are presented in Fig. 3. The reflectivity curves shows that the oxide film (105 nm) deposited on PS ARC improves the reflectivity of 55%, compared to the single layer PS ARC, leading to an effective reflectance of 3.8% in the 400-1000 nm wavelength range. However the optimised SiN_x film (45 nm) deposited on PS ARC is less efficient and improves the effective reflectance around 12%.

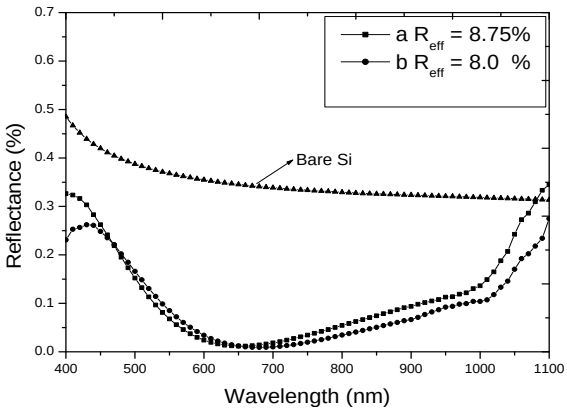

Figure 2 Total reflectance spectra of : (a) PS growth in HF (48 %): C_2H_5OH = 3:1, J = 20 mA/cm^2, t=6 s; (b) HF (48%): C_2H_5OH = 4:1, J = 20 mA/cm^2, t=6 s.

Sterhlke and co-workers have reduced the effective reflectivity to 2.7 % by using double layers PS ARC with a total thickness of 160 nm in the range 400-1000 nm [26]. However such a thickness of PS may risk to degrade the properties of the underlying n^+ emitter of the solar cell, which is generally 300 nm-thick. On the other hand the best result obtained in the literature for a double SiN_x/SiO_x ARC layer on polished silicon is R_{eff} = 6.3% in the range λ=400-1000 nm [23].

3.2 Surface passivation results We have shown that a low reflectivity can be obtained using PS/SiN_x:H and PS/SiO_x structures leading to an increase in the photogenerated current. We must then study the effect of such structures on the electrical performances of the solar cell. The photovoltaic pseudo-parameters V_{oc} and FF obtained with different structures are presented in Fig. 4.

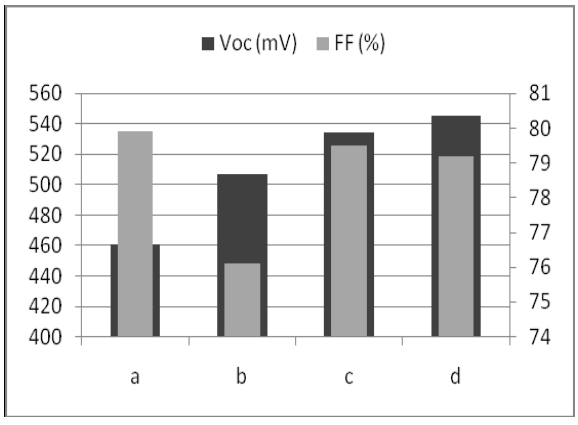

Figure 4 Parameters suns-V_{oc} obtained in a junction respectively before and after RTA with PS before (a) and after (b) annealing, (c) PS/SiO_x, (d) PS/SiN_x.

The values show that the silicon nitride and oxide films deposited on the PS layers partly improve the surface passivation, leading to an increase of V_{oc}, from 460 to 545 mV. This passivation enhancement is related to the high content of hydro-gen in the SiN_x:H layers: H diffuses within the thin PS layer and passivates the dangling bonds. In fact the Si-H bonds are strongly correlated to the passivation quality and can be used as surface passivation indicators [23]. The improvement of the V_{oc} value caused by the oxide films can be explained by the presence of the Si-O bonds which passivates the dangling bond within PS. The SiO_x also contains around 4% atomic of hydrogen [27], which diffuses within the PS-Si layer and increases the number of Si-H bonds which is initially formed during the formation of PS [17], thus enhancing the surface passivation of the pores.

We have also compared the V_{oc} values for the PS layer before and after an annealing step carried out in a halogen lamps furnace at 800° C for 30 s. An increase of the V_{oc} value from 461 mV to 507 mV is observed, which could be related to the improvement of the surface passivation quality. However this treatment degrades the pseudo fill factor FF, and requires a better optimization of the annealing step. The pseudo-Fill factor is of 79.1% for the PS layer, it decreases slightly for the PS/SiO_x and the PS/SiN_x structures in comparison with the pseudo-FF mentioned in the literature (~81%) [28], indicating that no serious recombination problem in the space-charge region existed and there was also no pronounced shunting, which confirms that the diode quality is excellent for all the structures.

In order to further investigate the impact of the dielectric layers on the surface passivation, we have performed FTIR analysis of the different structures (PS, PS/SiN_x and PS/SiO_x). The spectra were obtained with a Vertex 80 FTIR spectrometer, and are presented in Fig. 5.

The band in the 1040-1150 cm^{-1} range is assigned to the stretching vibration mode Si-O [29-31]. A clear increase of this intensity peak is observed for the PS/SiO_x layer, which is related to the high oxygen content in this layer, which contributes to the surface passivation. In addition a strong Si-N resonance is also observed between 830-860 cm^{-1} (stretching mode with Si_3N_4) [29,31,32] in PS/SiN_x structure, related to the high nitrogen content of the SiN.

On the other hand the relatively weak peak Si-H observed at 870 cm^{-1} bending vibration [33] in PS/SiO_x and PS/SiN_x show that the major part of hydrogen is diffused into the PS interface, and the dangling bonds Si-H are substituted by the compact Si-O and Si-N dangling bonds leading to an improvement of the surface passivation. The peak Si-O in the range 1040-1150 cm^{-1} observed in the PS layers before and after annealing at T = 800 °C show the increase of Si-O bonds in the PS after RTA. However the Si-H peak at 870 cm^{-1} is decreased in the same structure, indicating the substitution of Si-H by the Si-O dangling bonds which is confirmed the improvement of the passivation PS films after annealing.

3.3 Photocurrent calculation Following these results, PC1D program [25] was used to estimate the values of the photocurrent. The cell structure used for the simulation is: thickness = 220 μm, resistivity = 2.5 Ωcm, emitter: n-type, $3x10^{20}$ cm^{-3}. We consider that the majority of the photons absorbed in the porous Si layer do not contribute to the photo-generated current. Consequently one must take into account the effective transmittance of the PS/SiO_x and PS/SiN_x stack (T=1-R-A) calculated for each samples for the evaluation of the photocurrent. The photocurrent values presented in the Table 1, compared with a polished silicon surface, shows an improvement nearly 43% and 49% respectively for the PS/SiNx (45 nm thick SiNx layer) and PS/SiO_x (105 nm thick SiO_x layer). This result can be explained essentially by the lower reflectivity obtained by this structures.

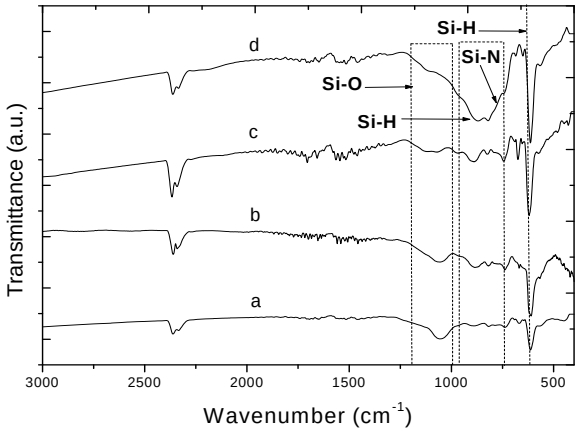

Figure 5 FTIR transmission spectra of structure (a) PS/SiO_x, (b) PS after annealing, (c) PS, (d) PS/SiN_x:H.

Table 1 $\Delta j_{sc}/j_{sc}$ was calculated in comparison with the n^+/p photo current J_{sc} corresponding to the non treated silicon surface.

Samples	R_{eff}(%)	J_{sc}(mA/cm^2)	$\Delta J_{sc}/J_{sc}$(%)
SiN(reference)	9.1	33.4	42.7
PS	8.0	29.8	27.4
PS/SiO_x	3.8	34.7	48.7
PS/SiN_x	7.0	33.4	42.7

4 Conclusion The deposition of the ARC SiO_x and SiN_x RF-PECVD was successfully carried out on porous silicon layer. Investigations of the reflection spectra showed that the optimum results can be obtained with electrochemical anodization of PS and RF-PECVD of SiO_x ARC layers. Effective reflectivity as low as 3.8% is obtained, which can lead to an expected improvement in short-circuit current of ~ 49%, compared to a bare silicon surface. The combination of porous silicon with dielectrics

layers allows to increase the surface passivation quality (Sun-V_{oc} increase of ~ 20%). We obtain thus better reflectivity results than with a double PS layer, with a minimisation of the surface degradation.

Acknowledgements The authors would like to thank the staff from the NanoLyon technical platform for helping in the realization of the structures.

References

[1] A. Prasad, S. Balakrishnan, S. K. Jain, and G. C. Jain, J. Electrochem. Soc. **192**, 596-598 (1982).
[2] G. Smestad, M. Kunst, and C. Vial, Sol. Energy Mater. Sol. Cells **26**, 277-283(1992).
[3] Y. S. Tsu, Y. Xiao, M. J. Heben, X. Wu, F. J. Pern, and S.K. Deb, In Conf. Rec., 23rd IEEE PVSC, Louis Ville, 1993, pp. 287-293.
[4] R. R. Bilyalov, L. Stalmans, L. Schirone, and C. Lévy-Clément, IEEE Trans. Electron. Devices **46**, 2035 (1999).
[5] C. Peckering, M. I. J. Beale, D. J. Robbins, P. J. Pearson, and R. Greef, J. Phys. C, Solid State Phys. **17**, 6335 (1984).
[6] R. R. Bilyalov, R. Lüdemann, W. Wettling, L. Stalmans, J. Poortmans, J. Nijs, L. Schirone, G. Sotgiu, S. Strehlke, and C. Lévy-Clément, Sol. Energy Mater. Sol. Cells **60**, 391 (2000).
[7] P. Menna, G. Di Francia, V. L. A Ferrara, Sol. Energy Mater. Sol. Cells **37**, 13 (1995).
[8] P. Vitanov, M. Delibasheva, E. Goranova, and M. Peneva, Sol. Energy. Mater. Sol. Cells **61**, 213 (2000).
[9] P. Vitanov, M. Goranova, N. Tyutyundzhiev, M. Delibasheva, E. Goranova, and P. Peneva, Thin Solid Films **279**, 299-303 (1997).
[10] S. Strehlke, S. Bastide, O. Polgar, M. Fried, and C. Lévy-Clément, J. Electrochem. Soc. **147**, 636-641 (2000).
[11] W. Theiss, S. Hilbrich, R. Arens-Fisher, M. G. Berger, H. Munder, in: Properties of Porous Silicon Nanostructures, edited by G. Amato, C. Delerue, and H. J. von Bardeleben, Vol. 5 (Gordon & Breach, London, 1997).
[12] D. W. Boeringer and R. Tsu, Appl. Phys. Lett **65**, 2332 (1994).
[13] B. Wang, D. Wang, L. Zhang, and T. Li, Thin Solid Films **293**, 40 (1997).
[14] A. Gupta, V. K. Jain, C. R, Jalwania, G. K. Singhal, O. P Arora, P. P. Puri, R. Singh, M. Pal, and V. Kumar, Semicond. Sci.Technol **10**, 698-702 (1995).
[15] V. M. Aroutiounian, K.H. Martirosyan, and P. Soukiassian, J. Phys. D: Appl. Phys **37**, L25-L28 (2004).
[16] A. Venkateswara, F. Ozanam, and J. N. Chazalviel, Electrochem. Soc. **138**, 153 (1991).
[17] R. Guerrero-Lemus, F. Ben-Hander, C. Hernàndez Rodriguez, and J. M. Martinez-Duart, Mater. Sci. Eng. B **101**, 249 (2003).
[18] C. Paillard, V. Paillard, A. Gagnaire, and J. Joseph, J. Noncryst. Soldis **216**, 77-82 (1997).
[19] P. Panek, K. Drabczyk, A. Focsa, and A. Slaoui, Mater. Sci. Eng. B **165**, 64 (2009).
[20] J. Dupuis, E. Fourmond, J. F. Lelièvre, D. Ballutaud, and M. Lemiti, Thin Solid Films **516**, 6954 (2008).
[21] I. Jozwik, P. Papet, A. Kaminski, E. Fourmond, F. Calmon, and M. Lemiti, J. Non-Cryst. Solids **354**, 4341 (2008).
[22] A. Cuevas and R. A. Sinton, Progr. Photovolt.: Res. Applications **5**(2), 79 (1997).
[23] J. Dupuis, J.-F. Lelièvre, E. Fourmond, V. Mong-The Yen, O. Nichiporuk, N. Le Quang, and M. Lemiti, in: 24th European Photovoltaic Solar Energy Conference Hamburg, Germany, 2009, pp.1633-1636.
[24] P. Nubile, Thin Solid Films **342**, 257 (1999).
[25] D. A. Clugston and P.A. Basore, Proc. of 26th IEEE Photovoltaic Spec. Conf., Anaheim, Californie, USA, 1997, pp. 207-210.
[26] S. Strehlke, S. Bastide, J. Guillet, and C. Lévy-Clément, Mater. Sci. Eng B **69/70**, 81 (2000).
[27] J. Dupuis, PhD Thesis, INSA-Lyon, France. 2009, p. 78.
[28] D. Kray, S. Hopman, A. Spiegel, B. Richerzhagen, and G. P. Willeke, Sol. Energy Mater. Sol. Cells **91**, 1638 (2007).
[29] P. V. Bulkin, P. L. Swart, and B. M. Lacquet. J. Non-Cryst. Solids **187**, 403 (1995).
[30] S. K. Ghosh and T. K. Hatwar, Thin Solid Films **166**, 359-(1988).
[31] S. Dreer and P. Wilhartitz, Pure Appl. Chem. **76**, 1161 (2004).
[32] R. F. Xiao, L. C. Ng, Ch. Jiang, Z. Yang, and G. K. L. Wong, Thin Solid Films **260**, 10 (1995).
[33] Y. Cros, N. Jaffrezic-Renault, J. M. Chovelon, and J. J. Fombon. J. Electrochem. Soc **139**, 507 (1992).